Proceedings of the Twenty-third (2013) International Offshore and Polar Engineering **www.isope.org**
Anchorage, Alaska, USA, June 30–July 5, 2013

ISBN 978-1-880653-99–9 (Set); ISSN 1098-6189 (Set)

Ice Age Classification Using Cross-Polarization Measurement with X-Band Radar

Armin Parsa
R&D Department, Rutter Inc.
St. John's, Newfoundland, Canada

ABSTRACT

The ability of X-band radar to differentiate young ice from second stage thin first-year ice (SST-FYI) is investigated. Cross-polarized X-band radar is employed on the Canadian Coast Guard Ship (CCGS) Henry Larsen, which is capable of measuring the depolarization characteristics of sea ice and glacial ice. The CCGS Henry Larsen recorded several hours of raw radar data (including the radar data of several ice states with both young ice and SST-FYI) on the Northeast Coast of Newfoundland during several days in March 2012. Based on the collected data, the depolarization characteristics of young ice and second stage thin first-year ice are analyzed for the grazing angles less than 4°. The results show that the depolarized reflected wave is stronger for the SST-FYI than the depolarized backscattered wave from the young ice.

KEY WORDS: Arctic ice; remote sensing; X-band radar; sea ice; polarization; target depolarization; ice characterization.

INTRODUCTION

Determination of safe ice routes is important for safe navigation of vessels in arctic regions. Following routes that have minimum ice concentration, vessels not only can maintain a safe journey, but also they can reduce the journey time and fuel consumption. Ice charts, which classify different ice concentration on a map, are often used for navigation, but they cannot be trusted when weather conditions are changing rapidly, which is often the case in arctic regions.

In recent years, polarimetric satellite synthetic aperture radar (SAR) has been used to classify the ice type and ice thickness based on the electromagnetic wave depolarization (Kim *et al.* 2012; Arkett *et al.* 2007). The MYI (multi-year ice) depolarizes the incident electromagnetic wave more than the FYI (first-year ice) due to lower salinity, allowing the waves to penetrate inside the MYI where they become depolarized by the air pockets and internal air bubbles.

Although ice classification has been made possible by satellite based remote sensing, satellite services are relatively expensive and they cannot provide real time imagery. Investigation has been started to develop ship-borne radar capable of providing real-time ice classification (Lewis *et al.* 1987; Orlando *et al.* 1990) which compares the reflected cross-polarized radar signal for MYI, FYI, and glacial ice. However, data acquisition and analysis of different FYI types have not been described in the literature yet.

This paper presents the experimental results obtained from the analysis of depolarized backscattered radar signal from the SST-FYI and young ice. The radar data used in this paper was collected on the Northeast Coast of Newfoundland by the CCGS Henry Larsen, in the period of March 15-17, 2012.

RADAR SETTINGS

A Cross-polarized X-band radar system, consisting of two radar antennas and two transceivers, was installed on the CCGS Henry Larsen during the trial as shown in Fig. 1, with the horizontal polarized antenna transmitting and receiving (HH) and the vertical polarized antenna receiving (HV) simultaneously. The main beams of the two antennas were synchronized so that they were always pointing in the same direction.

Fig. 2 shows the location of the CCGS Henry Larsen on March 16, 2012 where the radar data used for the analysis in this manuscript was recorded. The antenna and transceiver specifications of HH and HV radars are given in Table 1. The recorded images used in this manuscript were obtained when the antenna rotation speed was 120 rpm and the radars had Short Pulse transmission settings. As a result, the radar range resolution was 7.5 m for both channels. The antenna with vertical polarization had an antenna beamwidth of 2 degrees, while the beamwidth of the antenna with the horizontal polarization was 0.9 degrees. The beamwidth of the HV antenna was wider so that it could tolerate 1 degree error in angular synchronization. Since the HV antenna was in receive mode, the 0.9 degree illumination by the HH antenna defines the azimuth resolution of the HV channel. For data recording, Rutter's *sigma* S6 software had been used by the CCGS Henry Larsen. After digitizing the analog radar signal, *sigma* S6 stored each pixel with 12-bit depth (4096 intensity levels for representing the color intensity). Rutter's *sigma* S6 software was used during the analysis to replay the unprocessed recorded data and convert the radar data from polar to Cartesian coordinate format.

Fig. 1: (a) X-band radar system installed on the CCGS Henry Larsen which is capable of measuring co-polarized and cross-polarized radar return signal.

Fig. 2: Location of the CCGS Henry Larsen on the map at Northeast Coast Newfoundland.

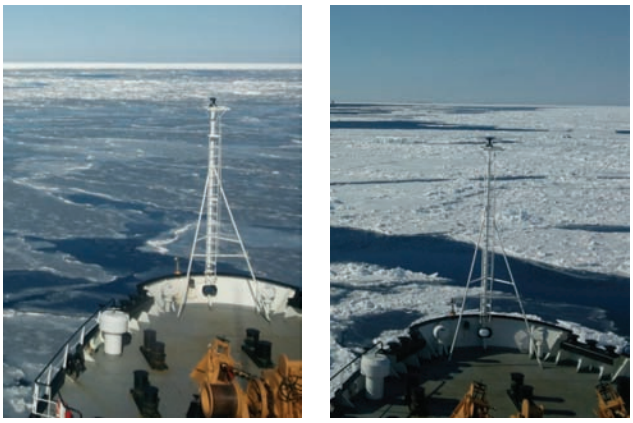

(a) (b)

Fig. 3: (a) Photograph of (a) young ice, (b) second stage thin first-year ice (SST-FYI) covered with snow.

DATA ANALYSIS

The recorded radar images of the HH and HV channels are used for the analysis. The recorded data which includes the depolarized backscattered radar data from both young ice and SST-FYI (Fig. 3) is chosen. According to Canadian Ice Service, the young ice, developing from nilas, has a thickness of 10-30 cm. Furthermore, the ice, in the developing stage between the young ice and the old ice, is called first-year ice. When the first-year ice thickness is 50-70 cm, the ice is defined as SST-FYI. Fig. 4 shows the ice chart provided by Canadian Ice Service on March 16th, which defines the types of sea ice captured during the radar recordings. In order to minimize any possible error (shift between the pixels of the two channels) originating from the horizontal displacement between the two radar antennas (HH and HV), we only use the samples in a 41x41 pixel square area for the analysis

Table 1: The radar system specification of HH and HV antenna and transceiver

	HV	HH
Antenna Gain (dB)	28	31
Antenna Polarization	Vertical	Horizontal
Antenna Beamwidth (degree)	2	0.9
Transmitter Peak Power (KW)	25	25
Operating Frequency (GHz)	9.41	9.41
Pulse Length (ns) [Short/Medium/Long]	50/250/750	50/250/750
IF Bandwidth (MHz) [Short Pulse]	20	20
Overall Noise Figure (dB) ≤	5	5
Side Lobes (dB) ≤	-30	-30
PRF (Hz) [Short/Medium/Long]	3000/1800/785	3000/1800/785
Antenna Rotation Speed (rpm)	30/45/60/120	30/45/60/120

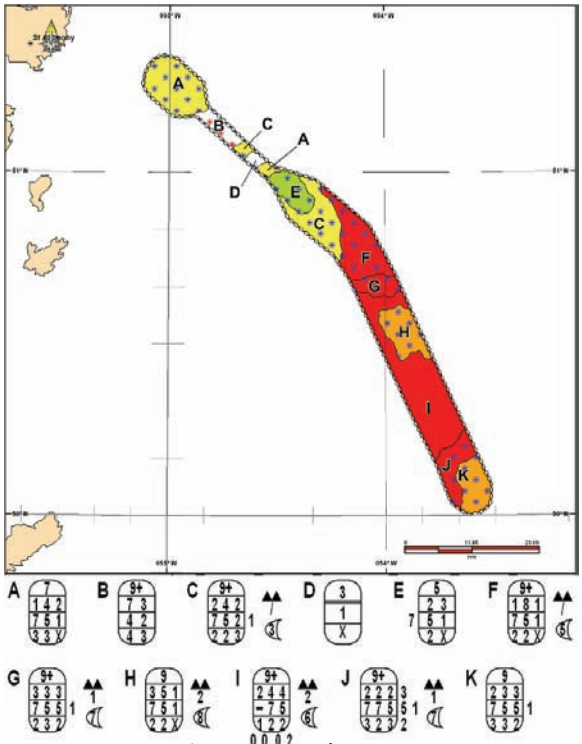

Fig. 4: Canadian ice chart[1] on March 16th, 2012 has characterized the young ice region (D) and SST-FYI (C) during the radar recordings.

[red square shown in Fig. 5(b)]. The square area location is always moving relative to ship's movement in a way that the center pixel of the sampling square is always along the ship's heading at 0.333 nmi range. As a result, the range and azimuth variation of the sampling pixels with respect to the antennas are minimized. Furthermore, the variation of the grazing angle of incidence for the sampled pixels is limited to angles between 2.5° to 3.1°.

To verify that the sampled pixels from the HH and HV channels were geometrically synchronized, the sampled pixels of the two channels

[1]The reproduction is a copy of an official work that is published by the Government of Canada and the reproduction has not been produced in affiliation with or with the endorsement of the Government of Canada. (Canadian Ice Service (CIS), Environment Canada, www.ec.gc.ca)

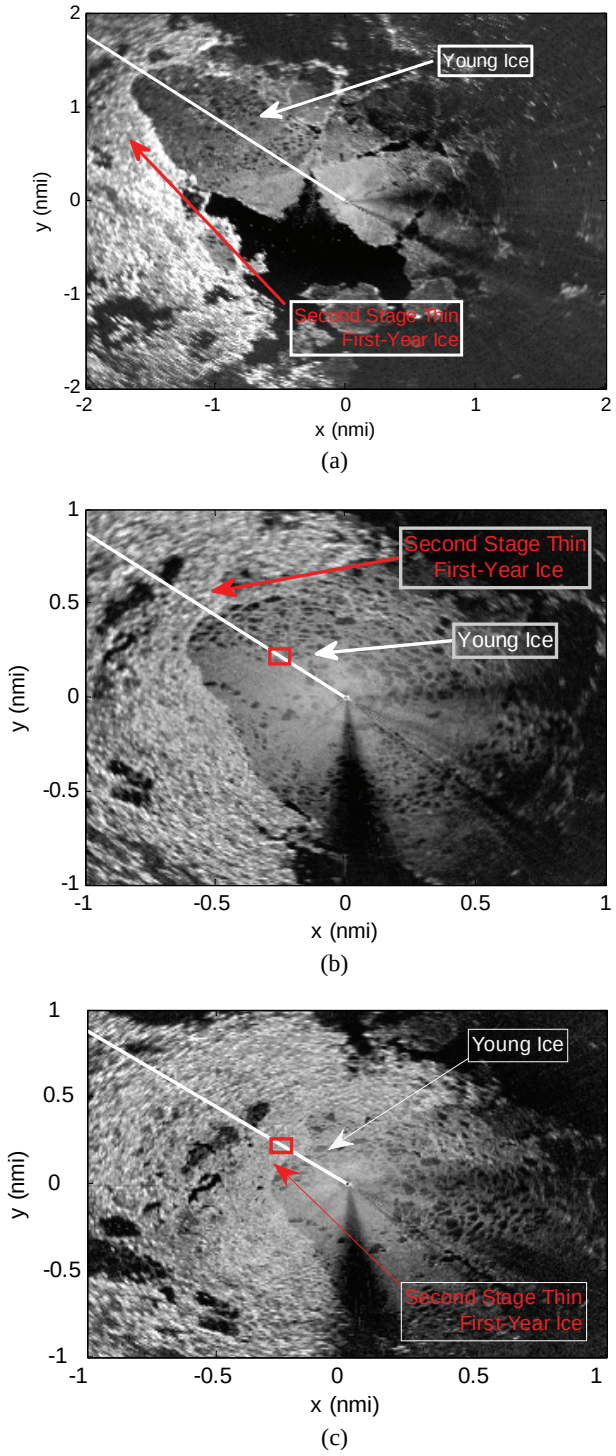

Fig. 5: (a) Radar image from co-polarized reflected wave (HH) recorded at time 16:49:04 GMT by the CCGS Henry Larsen at Northeast Newfoundland waters containing young ice and second stage thin first-year ice (SST-FYI). (b) Radar image from the depolarized reflected wave (HV) recorded at 16:57:54 GMT. The pixels inside the red square (41x41 area pixels) are sampling depolarized wave reflected from young ice. The center of the red square is always at 0.33 nmi range along the ship's heading direction (white line). (c) Depolarized wave (HV) reflected from the SST-FYI is sampled at 17:00:42 GMT by the red square.

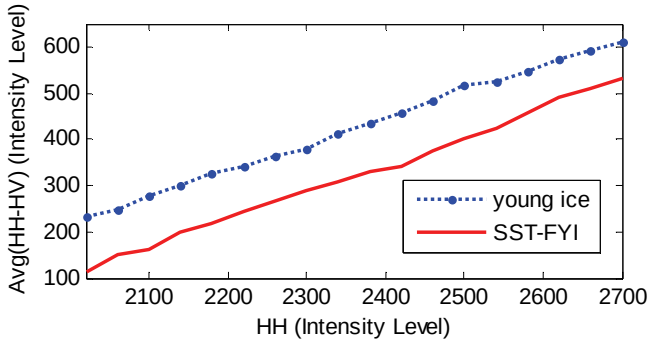

Fig. 6: Averaging HH-HV over 100 scans for each ice type. The young ice data was sampled from scans starting at time 16:56:15 GMT till 16:57:05 GMT, while SST-FYI data was extracted from the scans starting at 17:00:50 GMT to 17:01:40 GMT.

(HH and HV) were cross-correlated for several scans (images), and it was found that no geometrical shift was needed for synchronizing the sampled pixel locations of HH and HV channels. When replaying the data for analysis, the resolution of the image in rectangular coordinate format was 1024×1024 pixels, and maximum range setting was set to 1 nmi so that the radar image was covering an area of 2 nmi × 2 nmi. As a result, each pixel sampled for the analysis corresponds to 3.62 m. Fig. 5(a) shows the HH radar image (co-polarized reflected wave) recorded by the CCGS Henry Larsen at 16:49:04 GMT on March 16th. The areas containing two types of ice, namely young ice and SST-FYI, can be distinguished on the radar image. The amplitude of radar return signal by SST-FYI is higher than the backscattered wave by young ice since SST-FYI has a rougher surface than young ice. Although the ice features in this special case can be extracted by verifying the co-polarized amplitude of the radar return signals (HH channel only), we are interested in investigating the polarization effect by SST-FYI and young ice on the reflected signal. This information will be used in future in an ice type detection system which will be capable of classifying several types of ice in real-time, when the RCS signature of the ice (co-polarized amplitude) alone is not sufficient for ice type discrimination.

To better observe the difference between the cross-polarized signal of young ice and SST-FYI, the average of HH-HV is obtained for the data points with similar HH intensity levels as shown in Fig. 6 (the average is obtained for the HH-HV sample points with HH intensity in the proximity range of HH ± 20 for each HH intensity level on the x-axis). It is noted that 100 scans where used for generating the result shown in Fig. 6. The young ice data was sampled from scans starting at time 16:56:15 GMT till 16:57:05 GMT, while SST-FYI data was extracted from the scans starting at 17:00:50 GMT to 17:01:40 GMT. The result clearly shows that for the samples with similar HH intensity level, the HH-HV of young ice is larger than the HH-HV of SST-FYI. This indicates that SST-FYI depolarizes the incident wave more than young ice. Although the cross-polarized radar system on the CCGS Henry Larsen has not yet been calibrated, it is speculated from previous experience that 100 intensity level differences corresponds to 2.5 dB difference in received power. Only the data points with HH intensity level in the range 2000 to 2700 were used since most of the sampled points for SST-FYI had intensity levels greater than 2000 as shown in Fig. 7(a). Similarly, the intensity level of most of the young-ice data points were below 2700. Fig. 7(b) shows the histogram of the data points when the data points with HH intensity level in the range 1000 to 2700 are used. This kind of histogram might be misleading to the point that HH-HV for the young ice is smaller than the HH-HV for the SST-FYI. It is noted that the reflection by the SST-FYI is stronger than

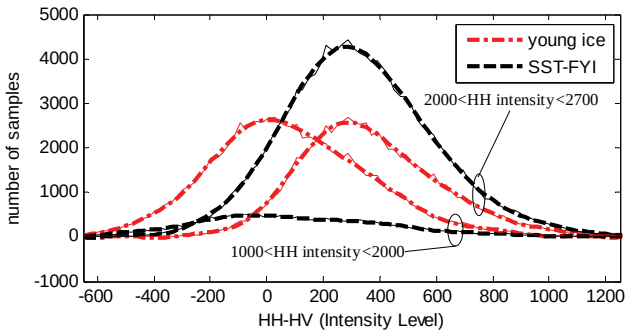

(a)

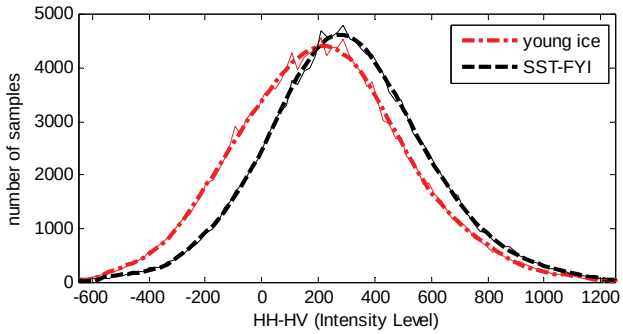

(b)

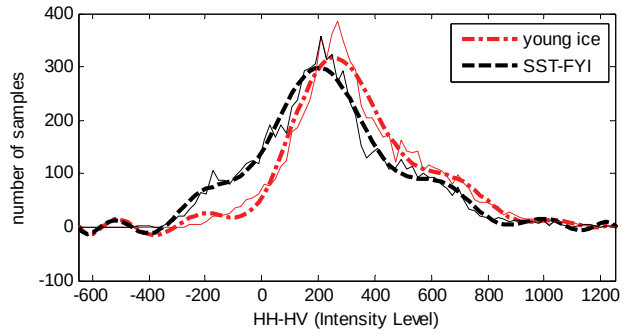

(c)

Fig. 7: Solid lines show the histograms, while dashed lines and dash-dotted lines show the fitted curves. (a) Histogram of the data points when 1000< HH intensity <2000 and 2000< HH intensity <2700. Young ice mean =367.8, SST-FYI mean= 329.1 when 2000< HH intensity <2700. Young ice mean =84, SST-FYI mean= 98.8 when 1000< HH intensity <2000. (b) Histogram of the data points when HH intensity satisfies 1000< HH intensity <2700, young ice mean =213.4, SST-FYI mean= 299.3. (c) Young ice mean =342.9, SST-FYI mean= 242.5 when 2200< HH intensity <2240.

the reflection by the young ice. As a result, the average HH intensity level of the SST-FYI is higher than that from the young ice. Since HH-HV intensity levels of data points increase directly as a function of HH (as shown in Fig. 6), the SST-FYI has more data points with higher HH-HV than young ice. In order to avoid such misinterpretation, the data points with close HH intensity levels must be compared. For example, Fig. 7(c) shows the histogram when the data points with HH intensity level in the range 2200 to 2240 only are filtered and selected. The result clearly show that young ice has more data points with larger HH-HV intensity level than SST-FYI (The SST-FYI depolarizes the incident wave more than young ice).

CONCLUSIONS

The ship-borne radar data collected by the CCGS Henry Larsen at Northeast Coast Newfoundland was used to study the polarization effect by young ice and SST-FYI. It was shown that the two types of ice could be differentiated and characterized by the curves representing the mean of HH-HV (the difference between the co-polarized and cross-polarized radar return signal) as a function of co-polarized (HH) signal intensity.

The only ground truth data available during this trial was the Canadian ice chart. In future, in order to fully study the mechanism involved with the cross-polarized radar for ice characterization, the ice surface roughness parameters should be measured during the ground-truth data collection. Further research is underway to fully understand and characterize the mechanism involved with the cross-polarized radar.

ACKNOWLEDGEMENTS

The author wishes to thank the Canadian Coast Guard for providing the recorded data, Desmond Smith, Stephen Hale, and Tom Healy for providing helpful comments and suggestions.

REFERENCES

Arkett, M, Flett, D, and Abreu, RD (2007). "C-band multiple polarization SAR for sea-ice monitoring – what can it do for the Canadian Ice Service," *Proc of Envisat Symposium*, Montreux, Switzerland, pp 23–27.

Kim, JW, Kim, DJ, Hwang, BJ (2012). "Characterization of arctic sea ice thickness using high-resolution spaceborne polarimetric SAR data," *IEEE Trans Geosci Remote Sensing*, Vol 50, pp 13-22.

Lewis, EO, Currie, BW, Haykin, SS (1987). *Detection and classification of ice*, Research Studies Press, Electronic & electrical engineering research studies, Radar and Sonar Series 1, 325 pp.

Orlando, JR, Mann, R, Hatkin, S (1990). "Classification of sea-ice images using a dual-polarized radar," *IEEE Journal of Oceanic Engineering*, Vol 15, No 3, pp 228-237.

Sigma S6 Ice Navigator Radar Processor (2010). [online] Available: http://www.rutter.ca